Title

Selective removal of natural caries lesions from dentin and tooth occlusal surfaces using a diode-pumped Er:YAG laser

Authors

Jew, Jamison
Chan, Kenneth H
Darling, Cynthia L
et al.

Publication Date

2017-02-08

DOI

10.1117/12.2256728

Peer reviewed

HHS Public Access

Author manuscript

Proc SPIE Int Soc Opt Eng. Author manuscript; available in PMC 2017 April 25.

Published in final edited form as:

Proc SPIE Int Soc Opt Eng. 2017 January 28; 10044: . doi:10.1117/12.2256728.

Selective removal of natural caries lesions from dentin and tooth occlusal surfaces using a diode-pumped Er:YAG laser

Jamison Jew, **Kenneth H. Chan**, **Cynthia L. Darling**, and **Daniel Fried**

University of California, San Francisco, San Francisco, CA 94143-0758

Abstract

Selective removal of caries lesions with high precision is best accomplished using lasers operating at high pulse repetition rates utilizing small spot sizes. Conventional flash-lamp pumped Er:YAG lasers are poorly suited for this purpose, but new diode-pumped solid-state (DPSS) Er:YAG lasers have become available operating at high pulse repetition rates. Microradiography was used to determine the mineral content of the demineralized dentin of 200-μm thick sections with natural caries lesions prior to laser ablation. The purpose of this study was to explore the use of a DPSS Er:YAG laser for the selective removal of demineralized dentin and natural occlusal lesions on extracted teeth.

Keywords

Er:YAG laser; dental caries; near-IR imaging; selective laser ablation

1. INTRODUCTION

DPSS Er:YAG lasers with high pulse repetition rates are more suitable for the selective removal of dental caries than existing Er:YAG lasers [1]. The flash-lamp pumped erbium solid-state lasers presently being used for dental hard tissue ablation are not suitable for this approach since they utilize high energy pulses and relatively low pulse repetition rates. Diode pumped Er:YAG lasers are now available operating with pulse repetition rates as high as 1–2 kHz and initial studies have been carried out demonstrating their utility for the ablation of dental hard tissues and bone [2–4]. Last year we investigated the use of this laser for the selective removal of caries lesions in the enamel [1].

For selective removal, low energy pulses and small spot sizes must be used to minimize the amount of tissue removed per laser pulse, therefore the laser has to be operated at high pulse repetition rates for practical removal rates. In addition the laser needs to be integrated with a scanner. Computer control is now feasible due to the recent advances in compact high-speed laser scanning technology such as MEMS (Micro-Electro-Mechanical Systems) mirrors and miniature galvanometer “galvo” based scanners. One approach is to remove the lesion layer by layer, i.e. image the lesion then scan the laser and remove an outer layer of the lesion, then re-image and scan again, repeating that process until the lesion is completely removed.

Therefore, it is advantageous to couple the laser with an imaging system for further selectivity. Image-guided laser ablation of dental caries requires the rapid acquisition of

high-contrast images of areas of enamel and dentin demineralization that can be input into the laser-scanning system to selectively remove areas of demineralization. Previous approaches for guiding laser ablation have included fluorescence [5–7] and near-IR transillumination [8]. Near-IR reflectance imaging is ideally suited for acquiring high-contrast images for image guided ablation due to the weak light scattering from sound enamel and the lack of interference from stains [9–11]. Stains which greatly interfere with visible light based methods do not interfere at near-IR wavelengths beyond 1300-nm, this is why visible reflectance measurements and fluorescence are of limited effectiveness in tooth occlusal surfaces [12, 13] and are not well-suited for image guided laser ablation. In previous studies we showed that near-IR reflectance in the wavelength regions coincident with increased water absorption namely 1450-nm and wavelengths higher than 1500-nm were ideally suited for this approach [14–16]. An important concern, essential for image-guided ablation, was that thermal modification of sound and demineralized tooth surfaces by the laser, could increase reflectivity from irradiated areas adversely influencing the lesion contrast and performance. We measured the lesion contrast at 1450-nm and from 1500–1700-nm before and after CO_2 laser ablation had been initiated and those changes were acceptable [17]. The enamel surfaces appear much rougher after Er:YAG ablation than they do after CO_2 laser ablation [1] and that may prevent the use of NIR reflectance imaging with the Er:YAG laser for image-guided ablation on enamel surfaces.

The purpose of this study was to explore the use of a DPSS Er:YAG laser for the selective removal of dentin and natural occlusal lesions on extracted teeth.

2. MATERIALS AND METHODS

2.1 Sample Preparation

Human tooth samples were divided into two groups (Fig. 1). Group 1 consisted of human tooth samples with dentinal lesions that were used for mineral content analysis. Group 2 consisted of whole teeth with occlusal lesions. Group 1 samples were prepared by cutting whole teeth into 200-μm slices using a IsoMet 5000 Precision Saw from Buehler (Lake Bluff, Il). Transverse Microradiography (TMR) was used on the slices to determine mineral content. A total of 9 samples were used for mineral content analysis. Group 2 samples were prepared by removing the roots of extracted teeth and mounting the crowns onto black orthodontic acrylic blocks. A total of 16 samples were used for laser ablation. The teeth were collected from dental offices in San Francisco Bay Area and sterilized with Gamma radiation.

2.2 Laser Setup and Parameters

Samples were irradiated using a DPSS Er:YAG laser, Model DPM-30 from Pantec Engineering (Liechtenstein) operating with a pulse duration of 50-μs. The laser energy output was monitored using a power meter EPM 1000, Coherent-Molectron (Santa Clara, CA), and the Joulemeter ED-200 from Gentec (Quebec, Canada). A high-speed XY-scanning system, Model ESP 301 controller with ILS100PP and VP-25AA stages from Newport (Irvine, CA) was used to scan the samples across the laser beam. The laser was focused to a spot size of ~150-μm using an aspheric ZnSe lens of 25 mm focal length. A

pressure air-actuated fluid spray delivery system consisting of a 780S spray valve, a Valvemate 7040 controller, and a fluid reservoir from EFD, Inc. (East Providence, RI) was used to provide a uniform spray of fine water mist onto the tooth surfaces at 2 mL/min.

For the Group 1 samples (dentin) the laser was operated with a pulse repetition rate of 100-Hz and the samples were scanned at a rate of 5 mm/sec. Fiducial squares 2 mm by 2 mm were created on each sample. Incisions were produced at a fluence of 10 J/cm^2 by one pass in one direction.

For the Group 2 samples (occlusal lesions), a rectangular box was cut across the lesion on the enamel samples with the box size encompassing the entire lesion. Incisions were produced by scanning the laser at a rate of 20 mm/sec with a pulse repetition rate of 200 Hz. The laser was scanned in one direction and each scan was separated by 25-μm for each iteration (laser spot size 150-μm). A fluence of 50 J/cm^2 was used. The iterations were repeated until the lesion was completely removed inside the box.

2.3 Digital Microscopy (DCDM)

Tooth surfaces were examined before and after laser irradiation using an optical microscopy/3D surface profilometry system, the VHX-1000 from Keyence (Elmwood, NJ). The VH-Z100R lens with a magnification of 100x-1000x. Depth composition digital microscopy images (DCDM) and 3D images were acquired by scanning the image plane of the microscope and reconstructing a depth composition image with all points at optimum focus displayed in a 2D image. The Keyence 3D shaped measurement software, VHX-H3M, was used to correct the tilt of the sample and measure the variation in depth over the enamel in the ablated areas.

2.4 Digital Transverse Microradiography (TMR)

A custom-built digital TMR system was used to measure mineral loss in the different partitions of the Group 1 samples. A high-speed motion control system with Newport (Irvine, CA) UTM150 and 850G stages and an ESP300 controller coupled to a video microscopy and laser targeting system was used for precise positioning of the tooth samples in the field of view of the imaging system. The volume percent mineral for each thin section was determined by comparison with a calibration curve of X-ray intensity vs. sample thickness created using sound enamel sections of 86.3±1.9 vol.% mineral varying from 50 to 300 μm in thickness using image analysis software. The calibration curve was validated via comparison with cross-sectional microhardness measurements. The volume percent mineral was determined using microradiography for section thickness ranging from 50 to 300-μm highly correlated with the volume percent mineral determined using microhardness, r^2 = 0.99 [18]. Microradiography images were loaded onto Igor Pro. The images contain the percentage of mineral content at each pixel. The VHX-1000 digital microscope was used to measure the depths of the incisions. By matching the positions in the TMR images and the digital microscope the removal depth was measured for varying mineral content.

2.5 CP-OCT System (OCT)

A cross-polarization OCT system purchased from Santec (Komaki, Aichi, Japan) was used to acquire 3D tomographic images of the Group 2 occlusal lesions before and after removal. This system acquires only the cross-polarization image (CP-OCT), not both the cross and co-polarization images (PS-OCT). The device, Model IVS-300-CP, utilizes a swept laser source; Santec Model HSL-200-30 operating with a 33 kHz a-scan sweep rate. The interferometer is integrated into the handpiece which also contains the microelectromechancial (MEMS) scanning mirror and the imaging optics. This CP-OCT system can acquire complete tomographic images of a volume 6×6×7 mm in size in ~3 seconds. This system operates at a wavelength of 1,321 nm with a bandwidth of 111 nm with a measured axial resolution in air of 11.4 mm (3 dB). The lateral resolution is 80 μm ($1/e^2$) with a transverse imaging window of 6×6 mm and a measured imaging depth of 7 mm in air. The polarization extinction ratio was measured to be 32 dB. Image registration and volumetric measurements were carried out using Avizo software from FEI (Hillsboro, OR).

2.6 Polarized Light Microscopy (PLM)

After sample imaging was completed, approximately 200 μm thick serial sections were cut using an Isomet 5000 saw (Buehler, IL), for polarized light microscopy (PLM). PLM was carried out using a Meiji Techno RZT microscope (Meiji Techno Co., LTD, Saitama, Japan) with an integrated digital camera, Canon EOS Digital Rebel XT (Canon Inc., Tokyo, Japan). The sample sections were imbibed in water and examined in the brightfield mode with crossed polarizers and a red I plate with 500-nm retardation.

3. RESULTS AND DISCUSSION

3.1 Group 1 - Dentinal Lesions

Initial Er:YAG dentin ablation rates were assessed using Group 1 samples. PLM and TMR were used to confirm lesion presence. Incisions were produced on the Group 1 sections by repeated Er:YAG laser scans as shown in Fig. 2. The ablation depths were analyzed using DCDM. The results indicate that the ablation rate correlates with the mineral content and that the incisions are deeper in areas with lower mineral content. DCDM images show that the dentin and demineralized dentin were ablated without any apparent thermal or mechanical damage.

3.2 Group 2 - Teeth with Occlusal Lesions

Lesions were removed from tooth occlusal surfaces by scanning the Er:YAG laser over selected regions of interest. DCDM images were taken after every 1–2 iterations (laser scans). Figure 3 shows the DCDM images during treatment of one tooth at three different time points. Ablation was stopped after the lesion was removed. Figure 4 shows CP-OCT images of the same tooth before and after ablation. The PLM post-ablation image (not shown) of the sectioned sample shows that most of the lesion was removed.

3.3 Summary

Ablation of dental hard tissues was achieved using the Er:YAG laser operating at high pulse repetition rates with minimal peripheral thermal damage. In addition, since water is the primary absorber of Er:YAG radiation and demineralized areas are more porous and have a higher water content, the ablation rate is significantly higher for demineralized enamel [1] and dentin vs sound tissues. In the future we plan on publishing an expanded manuscript of these results including statistical analyses.

Acknowledgments

The authors would like to thank William Fried and Andrew Jang for their contributions. This work was supported by NIDCR Grant R01-DE19631.

References

1. Yan R, Chan KH, Tom H, Simon JC, Darling CL, Fried D. Selective removal of dental caries with a diode-pumped Er:YAG laser. Proc SPIE Vol. 2015; 9306:O1–8.
2. Stock K, Diebolder R, Hausladen F, Hibst R. Efficient bone cutting with the novel diode pumped Er:YAG laser system: in vitro investigation and optimization of the treatment parameters. Proc SPIE Vol. 2014; 8926:P1–6.
3. Stock K, Diebolder R, Hausladen F, Wurm H, Lorenz S, Hibst R. Primary investigations on the potential of a novel diode pumped Er:YAG laser system for bone surgery. Proc SPIE Vol. 2013; 8565:D1–8.
4. Stock K, Hausladen F, Hibst R. Investigations on the potential of a novel diode pumped Er:YAG laser system for dental applications. Proc SPIE Vol. 2012; 8208:D1–5.
5. Eberhard J, Bode K, Hedderich J, Jepsen S. Cavity size difference after caries removal by a fluorescence-controlled Er:YAG laser and by conventional bur treatment. Clinical Oral Investigations. 2008; 12(4):311–8. [PubMed: 18500542]
6. Eberhard J, Eisenbeiss AK, Braun A, Hedderich J, Jepsen S. Evaluation of selective caries removal by a fluorescence feedback-controlled Er:YAG laser in vitro. Caries Res. 2005; 39(6):496–504. [PubMed: 16251795]
7. Jepsen S, Acil Y, Peschel T, Kargas K, Eberhard J. Biochemical and morphological analysis of dentin following selective caries removal with a fluorescence-controlled Er:YAG laser. Lasers Surg Med. 2008; 40(5):350–7. [PubMed: 18563782]
8. Tao YC, Fried D. Near-infrared image-guided laser ablation of dental decay. J Biomedical Opt. 2009; 14(5):054045.
9. Bühler CM, Ngaotheppitak P, Fried D. Imaging of occlusal dental caries" (decay) with near-IR light at 1310-nm. Optics Express. 2005; 13(2):573–582. [PubMed: 19488387]
10. Jones G, Jones RS, Fried D. Transillumination of interproximal caries lesions with 830-nm light. Proc SPIE. 2004; 5313:17–22.
11. Jones RS, Huynh GD, Jones GC, Fried D. Near-IR Transillumination at 1310-nm for the Imaging of Early Dental Caries. Optics Express. 2003; 11(18):2259–2265. [PubMed: 19466117]
12. Borsboom PCF, ten Bosch JJ. Fiber-optic scattering monitor for use with bulk opaque material. Appl Optics. 1982; 21(19):3531–3535.
13. ten Bosch JJ, van der Mei HC, Borsboom PCF. Optical monitor of in vitro caries. Caries Res. 1984; 18:540–547. [PubMed: 6593126]
14. Chung S, Fried D, Staninec M, Darling CL. Multispectral near-IR reflectance and transillumination imaging of teeth. Biomed Opt Express. 2011; 2(10):2804–2814. [PubMed: 22025986]
15. Fried WA, Darling CL, Chan K, Fried D. High Contrast Reflectance Imaging of Simulated Lesions on Tooth Occlusal Surfaces at Near-IR Wavelengths. Lasers Surg Med. 2013; 45(8):533–541. [PubMed: 23857066]

16. Simon JC, Chan KH, Darling CL, Fried D. Multispectral near-IR reflectance imaging of simulated early occlusal lesions: variation of lesion contrast with lesion depth and severity. Lasers Surg Med. 2014; 46(3):203–15. [PubMed: 24375543]
17. LaMantia NR, Tom H, Chan KH, Simon JC, Darling CL, Fried D. High contrast optical imaging methods for image guided laser ablation of dental caries lesions. Proc SPIE Vol. 2014; 8929:P1–7.
18. Darling CL, Featherstone JDB, Le CQ, Fried D. An automated digital microradiography system for assessing tooth demineralization. Proc SPIE. 2009; 7162:1–7.

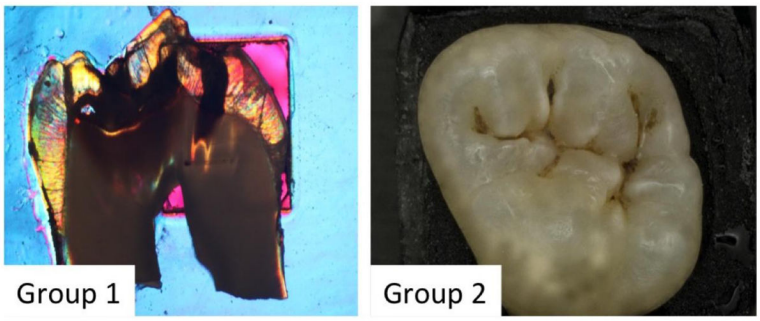

Fig. 1.
Images of teeth from each Group. Group 1 consisted of slices with dentinal lesions. Group 2 consisted of whole teeth with occlusal lesions.

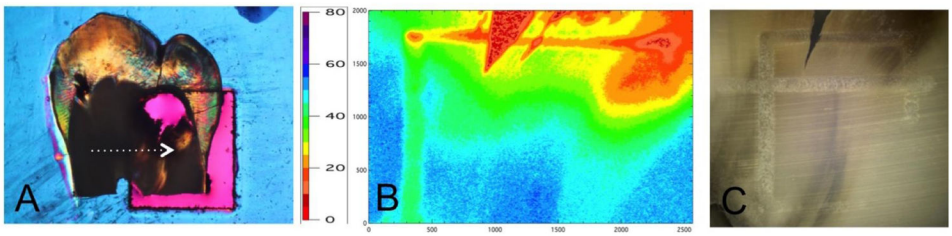

Fig. 2.

PLM, TMR, and DCDM images of one of the Group 1 dentin samples. (A) PLM image shows a sample mounted on a plastic slide with window. The white dotted line represents the path of the incision. (B) TMR image shows the varying mineral content on the sample before incisions. The color bar indicates the mineral content at different regions of the sample. (C) DCDM image shows sample after laser incision.

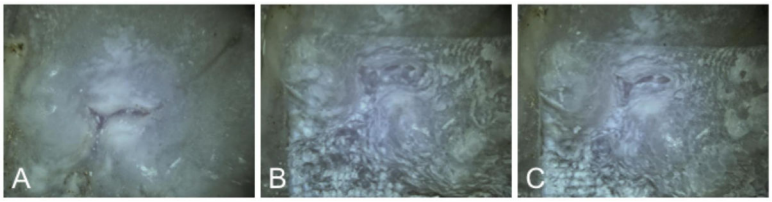

Fig. 3.

DCDM of one of the samples (Group 2) with an occlusal lesion at different time points during laser removal: (A) before ablation, after (B) 2 scans, and (C) 4 scans. The lesion in the center was removed after 4 scans.

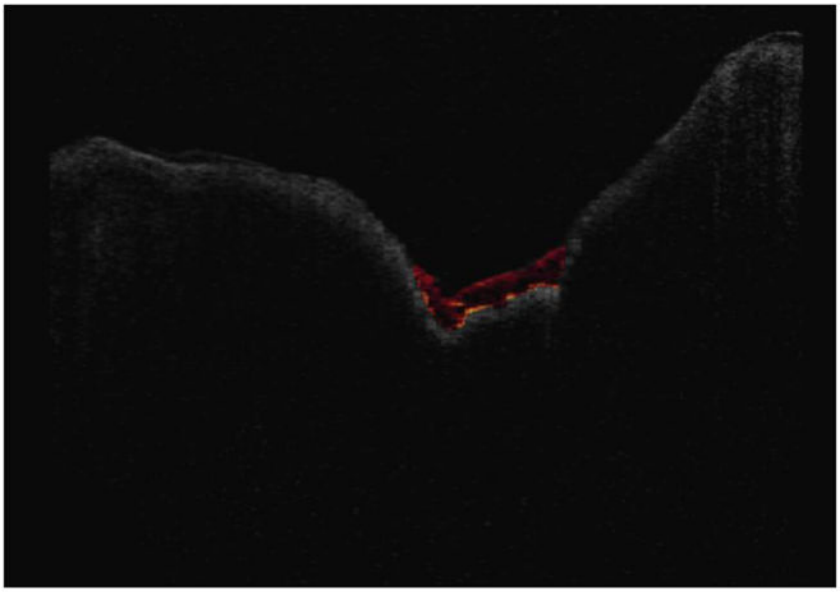

Fig. 4.
OCT b-scans of before and after removal of one of an occlusal lesions. The red scan is the sample before ablation.